FREQUENCY-SELECTIVE HYBRID PRECODING AND COMBINING FOR MMWAVE MIMO SYSTEMS WITH PER-ANTENNA POWER CONSTRAINTS

Javier Rodríguez-Fernández[†]*, Roberto López-Valcarce*[‡]*, and Nuria González-Prelcic*[†]

[†] The University of Texas at Austin. Email: {javi.rf,ngprelcic}@utexas.edu
[‡] atlanTTic Research Center, Universidade de Vigo, Spain. Email: valcarce@gts.uvigo.es

ABSTRACT

Configuring hybrid precoders and combiners is the main challenge to be solved to operate at millimeter wave (mmWave) frequencies. The use of hybrid architectures imposse hardware constraints on the analog precoder that need to be carefully dealt with. In this paper, we develop hybrid precoders and combiners aiming at minimizing the Euclidean distance with respect to the approximate all-digital precoders and combiners maximizing the spectral efficiency under per-antenna power constraints. Numerical results demonstrate the effectiveness of the proposed design method, whose performance is close to that of the all-digital solution.

Index Terms— mmWave, precoder and combiner design, MIMO, hybrid architecture

1. INTRODUCTION

Antenna array configuration is a challenging problem at hybrid mmWave Multiple-Input Multiple-Output (MIMO) systems. In frequency-selective scenarios, most of prior work pursues a hybrid factorization of a predefined all-digital solution into an analog precoder and a baseband precoder, which can be different for every subcarrier when a MIMO-OFDM framework is considered [1], [2], [3], [4], [5], [6], [7], [8], [9]. These papers, however, design the hybrid precoders with constraints on the total transmit power budget. This strategy has the problem that there is no control as to the amount of power that is delivered to a given antenna, and thus power backoff techniques are needed to meet the individual power constraints that are set by each antenna. This results in a reduction in power efficiency, which leads to lower spectral efficiency as well.

To the best of our knowledge, only [10], and [11] deal with the problem of hybrid precoding and/or combining with per-antenna power constraints at mmWave frequencies but under a narrowband channel model assumption. In the frequency-selective scenario, only [12] considers this problem and generalizes prior work in [11] for an OFDM/SC-FDE communications system.

In this paper, we present a novel low-complexity strategy to design hybrid precoders and combiners in a MIMO-OFDM/SC-FDE system under per-antenna power constraints. Unlike [12], we propose to optimize the Euclidean distance between the given all-digital precoder and its hybrid counterpart as a means to reduce the computational complexity of the design method. In the numerical results, we demonstrate the performance of the proposed design criterion, and highlight the importance of considering per-antenna power constraints in mmWave frequency-selective MIMO systems.

2. SYSTEM MODEL

We consider a single-user OFDM based hybrid mmWave MIMO link employing K subcarriers to send a vector of $N_{\rm s}$ data streams $\mathbf{s}[k] \in \mathbb{C}^{N_{\rm s}\times 1}$ using a transmitter with $N_{\rm t}$ antennas and a receiver with $N_{\rm r}$ antennas. It is assumed that $\mathbb{E}\{\mathbf{s}[k]\mathbf{s}^*[k]\} = \frac{P_{\rm t}}{N_{\rm s}}\mathbf{I}_{N_{\rm s}}$, with $P_{\rm t}$ being the transmit power. Both transmitter and receiver are assumed to employ fully-connected phase-shifter-based hybrid MIMO architectures, as shown in Fig. 1, with $L_{\rm t}$ and $L_{\rm r}$ RF chains, respectively. At the transmitter side, a frequency-selective hybrid precoder $\mathbf{F}[k] \in \mathbb{C}^{N_{\rm t}\times N_{\rm s}}$ is used, with $\mathbf{F}[k] = \mathbf{F}_{\rm RF}\mathbf{F}_{\rm BB}[k]$, $k = 0,\ldots,K-1$, where $\mathbf{F}_{\rm RF}$ is the analog precoder and $\mathbf{F}_{\rm BB}[k]$ its digital counterpart.

The MIMO channel between the transmitter and the receiver is assumed to be frequency-selective, having a delay tap length $N_{\rm c}$. Let $\rho_{\rm L}$ be the pathloss between transmitter and receiver; C, R_c be the number of clusters and rays within c-th cluster; $T_{\rm s}$ be the sampling period; $p_{\rm rc}(\tau)$ be a filter including the effects of pulse-shaping and other analog filtering evaluated at τ; $\alpha_{c,r} \in \mathbb{C}$ be the complex gain of the (c,r)-th path; $\tau_{c,r} \in \mathbb{R}$ be the delay of the (c,r)-th path; $\phi_{c,r} \in [0,2\pi)$ and $\theta_{c,r} \in [0,2\pi)$ be the angles-of-arrival and departure (AoA/AoD) of the (c,r)-th path, and $\mathbf{a}_{\rm R}(\phi_{c,r}) \in \mathbb{C}^{N_{\rm r}\times 1}$, $\mathbf{a}_{\rm T}(\theta_{c,r}) \in \mathbb{C}^{N_{\rm t}\times 1}$ be the array steering vectors for the receive and transmit antennas. Then, the d-th delay tap of the

This material is based upon work supported in part by the National Science Foundation under Grant No. CNS-1702800 and a gift from Toyota.

Supported by Agencia Estatal de Investigación (Spain) and the European Regional Development Fund (ERDF) under project WINTER (TEC2016-76409-C2-2-R), and by Xunta de Galicia (Agrupación Estratéxica Consolidada de Galicia accreditation 2016-2019; Red Temática RedTEIC 2017-2018)

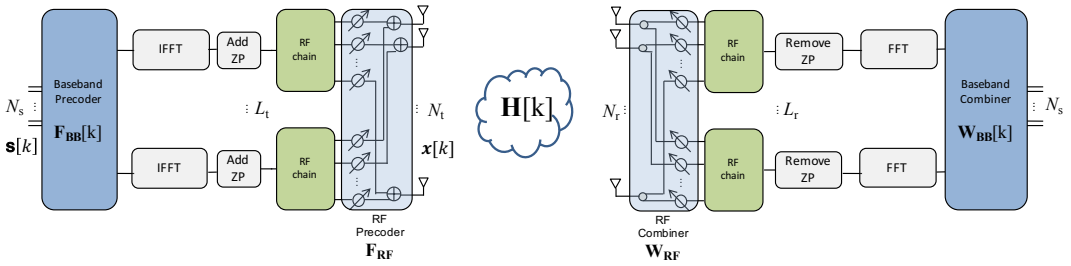

Fig. 1: Illustration of the structure of a hybrid MIMO architecture, which include analog and digital precoders and combiners.

channel is represented by a $N_{\rm r} \times N_{\rm t}$ matrix denoted as $\mathbf{H}_d$, $d = 0, \ldots, N_{\rm c}-1$, which, assuming a geometric channel model [13], can be written as

$$\mathbf{H}_d = \sqrt{\frac{N_{\rm t}N_{\rm r}}{\rho_{\rm L}\sum_{c=1}^{C} R_c}} \sum_{c=1}^{C}\sum_{r=1}^{R_c} \alpha_{c,r} p_{\rm rc}(dT_{\rm s} - \tau_{c,r}) \times \\ \times \mathbf{a}_{\rm R}(\phi_{c,r})\mathbf{a}_{\rm T}^{*}(\theta_{c,r}), \quad (1)$$

The frequency-domain MIMO channel matrix at subcarrier k can be written in terms of the K-point DFT of (1) as [14]

$$\mathbf{H}[k] = \sum_{d=0}^{N_{\rm c}-1} \mathbf{H}_d e^{-{\rm j}\frac{2\pi k}{K}d} = \mathbf{A}_{\rm R}\mathbf{G}[k]\mathbf{A}_{\rm T}^{*}, \quad (2)$$

where $\mathbf{G}[k] \in \mathbb{C}^{\sum_{c=1}^{C} R_c \times \sum_{c=1}^{C} R_c}$ is diagonal with non-zero complex entries, and $\mathbf{A}_{\rm R} \in \mathbb{C}^{N_{\rm r}\times\sum_{c=1}^{C} R_c}$ and $\mathbf{A}_{\rm T} \in \mathbb{C}^{N_{\rm t}\times\sum_{c=1}^{C} R_c}$ have columns containing the receive and transmit array steering vectors evaluated at the actual AoA/AoD $\{\mathbf{a}_{\rm R}(\phi_{c,r})\}$ and $\{\mathbf{a}_{\rm T}(\theta_{c,r})\}$.

The receiver applies a linear hybrid combiner $\mathbf{W}[k] = \mathbf{W}_{\rm RF}\mathbf{W}_{\rm BB}[k] \in \mathbb{C}^{N_{\rm r}\times N_{\rm s}}$, with $\mathbf{W}_{\rm RF} \in \mathbb{C}^{N_{\rm r}\times L_{\rm r}}$ being the analog combiner, and $\mathbf{W}_{\rm BB}[k] \in \mathbb{C}^{L_{\rm r}\times N_{\rm s}}$ its baseband counterpart. Under the assumption of perfect time-frequency synchronization, the received signal at subcarrier k becomes

$$\mathbf{y}[k] = \mathbf{W}_{\rm BB}^{*}[k]\mathbf{W}_{\rm RF}^{*}\mathbf{H}[k]\mathbf{F}_{\rm RF}\mathbf{F}_{\rm BB}[k]\mathbf{s}[k] + \mathbf{n}[k], \quad (3)$$

where $\mathbf{n}[k] \sim \mathcal{N}\left(0, \sigma^2\mathbf{W}_{\rm BB}^{*}[k]\mathbf{W}_{\rm RF}^{*}\mathbf{W}_{\rm RF}\mathbf{W}_{\rm BB}[k]\right)$ is the circularly symmetric complex Gaussian distributed additive noise vector.

3. PROPOSED DESIGN

In this section, we present a novel low-complexity algorithm to design hybrid precoders and combiners accounting for practical per-antenna power constraints. The derivation of the approximate all-digital precoders and combiners maximizing the spectral efficiency ca be found in [12]. Henceforth, we will assume the all-digital precoders and combiners are known, and thus our attention will be focused on the hybrid factorization problem with per-antenna power constraints.

3.1. Hybrid precoder design

In [12], the hybrid factorization of the all-digital precoders is based on the minimization of the chordal distance between the all-digital precoders and their hybrid counterparts. Here we propose instead to minimize their Euclidean distance, since in that way a less complex solution can be obtained, as shown next.

Let $\mathcal{M}^{N_{\rm t}\times L_{\rm t}}(Q_{\rm t})$ denote the set of $N_{\rm t} \times L_{\rm t}$ matrices with unit-magnitude entries and phases taken from a discrete set $\mathcal{A}(Q_{\rm t}) = \{0, \frac{2\pi}{2^{Q_{\rm t}}}, \ldots, \frac{2\pi(2^{Q_{\rm t}}-1)}{2^{Q_{\rm t}}}\}$, with $Q_{\rm t}$ denoting the number of quantization bits. Also, let p_j be the maximum available power budget for the j-th transmit antenna, $1 \le j \le N_{\rm t}$. Let us consider a set of all-digital precoders $\{\mathbf{F}[k] \in \mathbb{C}^{N_{\rm t}\times N_{\rm s}}\}_{k=0}^{K-1}$, and define the following matrices

$$\mathbf{F} \triangleq \left[\mathbf{F}[0]\cdots\mathbf{F}[K-1]\right], \quad (\text{size } N_{\rm t} \times N_{\rm s}K) \quad (4)$$

$$\mathbf{F}_{\rm BB} \triangleq \left[\mathbf{F}_{\rm BB}[0]\cdots\mathbf{F}_{\rm BB}[K-1]\right], \quad (\text{size } L_{\rm t} \times N_{\rm s}K). \quad (5)$$

Then, the problem of finding $\mathbf{F}_{\rm RF}$ and $\{\mathbf{F}_{\rm BB}[k]\}_{k=0}^{K-1}$ subject to per-antenna power constraints can be stated as

$$\min_{\mathbf{F}_{\rm RF},\mathbf{F}_{\rm BB}} \|\mathbf{F} - \mathbf{F}_{\rm RF}\mathbf{F}_{\rm BB}\|_F^2 \quad (6)$$

$$\text{subject to} \quad \begin{cases} \mathbf{F}_{\rm RF} \in \mathcal{M}^{N_{\rm t}\times L_{\rm t}}(Q_{\rm t}), \\ \frac{1}{N_{\rm s}}\mathbf{e}_j^{*}\left(\mathbf{F}_{\rm RF}\mathbf{F}_{\rm BB}\mathbf{F}_{\rm BB}^{*}\mathbf{F}_{\rm RF}^{*}\right)\mathbf{e}_j \le p_j, \\ j = 1, \ldots, N_{\rm t}, \end{cases}$$

The optimization problem in (6) is non-convex due to the hardware constraints imposed by the hybrid architecture, which are parameterized by the discrete set $\mathcal{M}^{N_{\rm t}\times L_{\rm t}}(Q_{\rm t})$. Due to this, we propose to first obtain a reasonable approximation for $\mathbf{F}_{\rm RF}$, and then design $\mathbf{F}_{\rm BB}[k]$ to minimize (6).

Let us consider an SVD of $\mathbf{F} = \mathbf{U}_F\mathbf{\Sigma}_F\mathbf{V}_F^{*}$, with $\mathbf{U}_F \in \mathbb{C}^{N_{\rm t}\times{\rm rank}\{\mathbf{F}\}}$, $\mathbf{\Sigma}_F \in \mathbb{C}^{{\rm rank}\{\mathbf{F}\}\times{\rm rank}\{\mathbf{F}\}}$, $\mathbf{V}_F \in \mathbb{C}^{{\rm rank}\{\mathbf{F}\}\times N_{\rm s}K}$, with the singular values in $\mathbf{\Sigma}_F$ sorted in decreasing order. Also, let us momentarily ignore the constraints in (6) and find an unconstrained solution $\tilde{\mathbf{F}}_{\rm RF}$, $\tilde{\mathbf{F}}_{\rm BB}$ to (6). This is a low-rank approximation problem, and by the Eckart-Young theorem the solution is given by $\tilde{\mathbf{F}}_{\rm RF}\tilde{\mathbf{F}}_{\rm BB} = \mathbf{U}_{F,1}\mathbf{\Sigma}_{F,1}\mathbf{V}_{F,1}^{*}$, where $\mathbf{U}_{F,1} \in \mathbb{C}^{N_{\rm t}\times L_{\rm t}}$, $\mathbf{V}_{F,1} \in \mathbb{C}^{N_{\rm s}K\times L_{\rm t}}$ are the matrices comprising the first $L_{\rm t}$ columns of $\mathbf{U}_F$ and $\mathbf{V}_F$, and $\mathbf{\Sigma}_{F,1} \in \mathbb{C}^{L_{\rm t}\times L_{\rm t}}$ is diagonal comprising the first $L_{\rm t}$ singular values of $\mathbf{\Sigma}_F$. Then, $\tilde{\mathbf{F}}_{\rm RF}$, $\tilde{\mathbf{F}}_{\rm BB}$ are given by $\tilde{\mathbf{F}}_{\rm RF} =$

$\mathbf{U}_{F,1}\mathbf{A}$, $\tilde{\mathbf{F}}_{\text{BB}} = \mathbf{A}^{-1}\mathbf{\Sigma}_{F,1}\mathbf{V}_{F,1}^*$, for an arbitrary invertible $\mathbf{A} \in \mathbb{C}^{L_\text{t}\times L_\text{t}}$. Although this provides a closed-form solution for $\mathbf{F}_{\text{RF}}$, $\mathbf{F}_{\text{BB}}$, we need to take into account both the per-antenna and hardware constraints. The analog precoder $\mathbf{F}_{\text{RF}}$ is taken as the closest element (in Euclidean distance) of the feasible set $\mathcal{M}^{N_\text{t}\times L_\text{t}}(Q_t)$ to $\tilde{\mathbf{F}}_{\text{RF}}$, which is readily found to be $[\mathbf{F}_{\text{RF}}]_{j,i} = e^{\text{j}Q\left(\measuredangle[\tilde{\mathbf{F}}_{\text{RF}}]_{j,i}\right)}$, $1 \le j \le N_\text{t}$, $1 \le i \le L_\text{t}$, with $Q(\measuredangle x)$ denoting the quantized phase of $x in \mathbb{C}$. It remains to design the baseband precoder $\mathbf{F}_{\text{BB}}$. At this point, the per-antenna power constraints need to be included to find an overall solution to the original problem in (6). Developing the cost in (6) yields

$$\begin{aligned}\|\mathbf{F}-\mathbf{F}_{\text{RF}}\mathbf{F}_{\text{BB}}\|_F^2 = \text{tr}\left\{\mathbf{F}\mathbf{F}^*\right\} + \text{tr}\left\{\mathbf{F}_{\text{BB}}{}^*\mathbf{F}_{\text{RF}}{}^*\mathbf{F}_{\text{RF}}\mathbf{F}_{\text{BB}}\right\} \\ - 2\,\text{Re}\left\{\text{tr}\left\{\mathbf{F}^*\mathbf{F}_{\text{RF}}\mathbf{F}_{\text{BB}}\right\}\right\}.\end{aligned} \tag{7}$$

If we assume that the power constraints in (6) are to be met with equality, then the second term in (7) is a constant given by $N_\text{s}\sum_{j=1}^{N_\text{t}} p_j$. Under such assumption, the only term in (7) that depends on $\mathbf{F}_{\text{BB}}$ is the last one. Let us now define the $L_\text{t} \times N_\text{s}K$ matrix $\mathbf{G} \triangleq \mathbf{F}_{\text{RF}}{}^*\mathbf{F}$ having SVD $\mathbf{G} = \mathbf{U}_G\mathbf{\Sigma}_G\mathbf{V}_G^*$, with $\mathbf{U}_G \in \mathbb{C}^{L_\text{t}\times L_\text{t}}$, $\mathbf{\Sigma}_G \in \mathbb{C}^{L_\text{t}\times L_\text{t}}$, $\mathbf{V}_G \in \mathbb{C}^{N_\text{s}K\times L_\text{t}}$. Let us also introduce an SVD of $\mathbf{F}_{\text{BB}} = \mathbf{U}_{\text{BB}}\mathbf{\Sigma}_{\text{BB}}\mathbf{V}_{\text{BB}}^*$, with $\mathbf{U}_{\text{BB}} \in \mathbb{C}^{L_\text{t}\times L_\text{t}}$, $\mathbf{\Sigma}_{\text{BB}} \in \mathbb{C}^{L_\text{t}\times L_\text{t}}$, $\mathbf{V}_{\text{BB}} \in \mathbb{C}^{N_\text{s}K\times L_\text{t}}$. Therefore, the problem of finding $\mathbf{F}_{\text{BB}}$ accounting for the per-antenna constraints can be stated as

$$\max_{\mathbf{U}_{\text{BB}},\mathbf{\Sigma}_{\text{BB}},\mathbf{V}_{\text{BB}}} \text{Re}\left\{\text{tr}\left\{\mathbf{G}^*\mathbf{F}_{\text{BB}}\right\}\right\} \tag{8}$$

$$\text{subject to} \quad \frac{1}{N_\text{s}}\mathbf{e}_j^*\left(\mathbf{F}_{\text{RF}}\mathbf{F}_{\text{BB}}\mathbf{F}_{\text{BB}}^*\mathbf{F}_{\text{RF}}^*\right)\mathbf{e}_j \le p_j, \tag{9}$$

$$j = 1,\ldots,N_\text{t}. \tag{10}$$

Solving (8)-(10) is still difficult. For this reason, we will neglect the influence of the per-antenna constraints on the singular vectors of $\mathbf{F}_{\text{BB}}$ in order to find a suboptimal solution to (8)-(10). Using Von Neumann's trace inequality [15], we can find an upper bound to the cost in (8) as follows:

$$\begin{aligned}\text{Re}\left\{\text{tr}\left\{\mathbf{G}^*\mathbf{F}_{\text{BB}}\right\}\right\} &\le \left|\text{tr}\left\{\mathbf{G}^*\mathbf{F}_{\text{BB}}\right\}\right| \\ &= \left|\text{tr}\left\{\mathbf{\Sigma}_G\mathbf{U}_G^*\mathbf{F}_{\text{BB}}\mathbf{V}_G\right\}\right| \\ &\le \text{tr}\left\{\mathbf{\Sigma}_G\mathbf{\Sigma}_{\text{BB}}\right\}.\end{aligned} \tag{11}$$

The upper bound in (11) is attained by setting $\mathbf{U}_{\text{BB}} = \mathbf{U}_G$ and $\mathbf{V}_{\text{BB}} = \mathbf{V}_G$. With this choice for the singular vectors, we now optimize the singular values under the per-antenna power constraints. Letting $\mathbf{g}_j \triangleq \mathbf{U}_{\text{BB}}^*\mathbf{F}_{\text{RF}}{}^*\mathbf{e}_j$, (8) boils down to

$$\max_{\{\sigma_{\text{BB},i}\}_{i=1}^{L_\text{t}}} \sum_{i=1}^{L_\text{t}} \sigma_{G,i}\sigma_{\text{BB},i} \tag{12}$$

$$\text{subject to} \quad \frac{1}{N_\text{s}}\sum_{i=1}^{L_\text{t}} |\text{g}_{j,i}|^2\sigma_{\text{BB},i}^2 \le p_j, \tag{13}$$

$$j = 1,\ldots,N_\text{t},$$

which is a linear program in the allocation variables $\{\sigma_{\text{BB},i}\}_{i=1}^{L_\text{t}}$ that can be efficiently solved using any convex optimization tool.

3.2. Hybrid combiner design

To design the hybrid combiner $\mathbf{W}[k] = \mathbf{W}_{\text{RF}}\mathbf{W}_{\text{BB}}[k]$, we pursue the optimization of the same metric as the one in (6). As analyzed in [12], choosing the combiner to have orthonormal columns preserves optimality in terms of spectral efficiency. Thus, given an all-digital combiner $\{\mathbf{W}[k]\}_{k=0}^{K-1}$, let us define the following matrices

$$\mathbf{W} \quad \triangleq \left[\mathbf{W}[0]\cdots\mathbf{W}[K-1]\right], \quad (\text{size } N_\text{r}\times N_\text{s}K) \tag{14}$$

$$\mathbf{W}_{\text{BB}} \quad \triangleq \left[\mathbf{W}_{\text{BB}}[0]\cdots\mathbf{W}_{\text{BB}}[K-1]\right], \quad (\text{size } L_\text{r}\times N_\text{s}K) \tag{15}$$

Then, the problem of designing $\mathbf{W}_{\text{RF}}$, $\{\mathbf{W}_{\text{BB}}[k]\}_{k=0}^{K-1}$ can be stated as

$$\min_{\mathbf{W}_{\text{RF}},\{\mathbf{W}_{\text{BB}}[k]\}} \sum_{k=0}^{K-1} \|\mathbf{W}[k]-\mathbf{W}_{\text{RF}}\mathbf{W}_{\text{BB}}[k]\|_F^2 \tag{16}$$

$$\text{subject to} \quad \begin{cases} \mathbf{W}_{\text{RF}} \in \mathcal{M}^{N_\text{t}\times L_\text{t}}(Q_\text{t}), \\ \mathbf{W}_{\text{BB}}^*[k]\mathbf{W}_{\text{RF}}^*\mathbf{W}_{\text{RF}}\mathbf{W}_{\text{BB}}[k] = \mathbf{I}_{N_\text{s}}, \\ k = 0,\ldots,K-1 \end{cases}$$

Analogously to the design of the hybrid precoder, we first seek a reasonable approximation for the RF combiner, and then optimize the baseband combiner $\mathbf{W}_{\text{BB}}$. Let us consider an SVD $\mathbf{W} = \mathbf{U}_W\mathbf{\Sigma}_W\mathbf{V}_W^*$, with $\mathbf{U}_W \in \mathbb{C}^{N_\text{r}\times\text{rank}\{\mathbf{W}\}}$, $\mathbf{\Sigma}_W \in \mathbb{C}^{\text{rank}\{\mathbf{W}\}\times\text{rank}\{\mathbf{W}\}}$, $\mathbf{V}_W \in \mathbb{C}^{N_\text{s}K\times\text{rank}\{\mathbf{W}\}}$. Then, if we momentarily ignore the constraints in (16), we can again invoke the Eckart-Young theorem to find that the unconstrained $\tilde{\mathbf{W}}_{\text{RF}}$, $\tilde{\mathbf{W}}_{\text{BB}}$ satisfy $\tilde{\mathbf{W}}_{\text{RF}}\tilde{\mathbf{W}}_{\text{BB}} = \mathbf{U}_{W,1}\mathbf{\Sigma}_{W,1}\mathbf{V}_{W,1}^*$. Then, setting $\tilde{\mathbf{W}}_{\text{RF}} = \mathbf{U}_{W,1}\mathbf{B}$ and $\tilde{\mathbf{W}}_{\text{BB}} = \mathbf{B}^{-1}\mathbf{\Sigma}_{W,1}\mathbf{V}_{W,1}^*$ satisfies the previous condition, for any invertible $\mathbf{B} \in \mathbb{C}^{L_\text{r}\times L_\text{r}}$. Now, similarly to the RF precoder, a sensible approach to design the RF combiner is to set $[\mathbf{W}_{\text{RF}}]_{m,n} = e^{\text{j}Q(\measuredangle[\tilde{\mathbf{W}}_{\text{RF}}]_{m,n})}$, $1 \le m \le N_\text{r}$, $1 \le n \le L_\text{r}$. With this design of the RF combiner, it remains to solve (16) as a function of $\mathbf{W}_{\text{BB}}[k]$. Let $\mathbf{W}_{\text{RF}} = \mathbf{U}_{\text{RF}}\mathbf{\Sigma}_{\text{RF}}\mathbf{V}_{\text{RF}}^*$ be an SVD of $\mathbf{W}_{\text{RF}}$. Now, the constraints in (16) can be rewritten as

$$\mathbf{W}_{\text{BB}}^*[k]\mathbf{V}_{\text{RF}}\mathbf{\Sigma}_{\text{RF}}^2\mathbf{V}_{\text{RF}}^*\mathbf{W}_{\text{BB}}[k] = \mathbf{I}_{N_\text{s}}, \quad k = 0,\ldots,K-1, \tag{17}$$

such that the optimum baseband precoder $\mathbf{W}_{\text{BB}}[k]$ is of the form $\mathbf{W}_{\text{BB}}[k] = \mathbf{V}_{\text{RF}}\mathbf{\Sigma}_{\text{RF}}^{-1}\mathbf{Z}_W[k]$, with $\mathbf{Z}_W[k] \in \mathbb{C}^{L_\text{r}\times N_\text{s}}$ a semi-unitary matrix. Then, it follows that $\mathbf{W}_{\text{RF}}\mathbf{W}_{\text{BB}}[k] = \mathbf{U}_{\text{RF}}\mathbf{Z}[k]$ and (16) becomes

$$\begin{aligned}\min_{\mathbf{Z}[k]} \sum_{k=0}^{K-1} \|\mathbf{W}[k]-\mathbf{U}_{\text{RF}}\mathbf{Z}_W[k]\|_F^2 \\ \text{subject to} \quad \mathbf{Z}_W^*[k]\mathbf{Z}_W[k] = \mathbf{I}_{N_\text{s}}.\end{aligned} \tag{18}$$

Problem (18) is recognized as an *orthogonal Procrustes problem* [16, p. 601], whose solution is as follows. Let $\mathbf{C}[k] \triangleq$

$\mathbf{U}_{\mathrm{RF}}^{*}\mathbf{W}[k]$, with SVD $\mathbf{C}[k] = \mathbf{U}_C[k]\mathbf{\Sigma}_C[k]\mathbf{V}_C^{*}[k]$. Then, the solution to (16) is $\mathbf{Z}_W[k] = \mathbf{U}_C[k]\mathbf{V}_C^{*}[k]$. This concludes the design of the hybrid combiner.

4. RESULTS

In this section, we provide numerical results on the performance of the proposed hybrid precoding and combining strategy with per-antenna power constraints (PPC). We focus on both the spectral efficiency and the per-antenna power consumption, thereby showing the relationship between these parameters. The SNR in the system is defined as $\mathrm{SNR} \triangleq P_{\mathrm{t}}/\sigma^2$, and $P_{\mathrm{t}} = 1$ for illustration. If we define the effective channel after combining, at the k-th subcarrier, as $\mathbf{H}_{\mathrm{ef}}[k] = \mathbf{W}^{*}[k]\mathbf{H}[k]\mathbf{F}[k]$, then the average achievable spectral efficiency is given by

$$\mathcal{R} = \frac{1}{K}\sum_{k=0}^{K-1} \log_2 \left| \mathbf{I}_{N_{\mathrm{s}}} + \frac{\mathrm{SNR}}{N_{\mathrm{s}}} \mathbf{H}_{\mathrm{ef}}[k]\mathbf{H}_{\mathrm{ef}}^{*}[k] \right|. \qquad (19)$$

We use the frequency-selective channel model in (1), with small-scale parameters obtained from the 3GPP Urban Macrocell (UMa) 5G channel model (NR) [17], which is implemented in QuaDRiGa channel simulator [18], [19]. The Rician factor is chosen to be -10 dB for illustration. The transmitter and receiver are equipped with Uniform Linear Arrays (ULA) having $N_{\mathrm{t}} = 64$ and $N_{\mathrm{r}} = 16$ antennas with $\lambda/2$ separation, respectively. The number of RF chains is set to $L_{\mathrm{t}} = 4$ and $L_{\mathrm{r}} = 2$. Results are averaged over 100 channel realizations, and $K = 64$ subcarriers are employed. Using the all-digital precoders developed in [12], we compare the proposed PPC design with the conventional all-digital precoders and combiners taken as the dominant right and left singular vectors of the channel, and power allocation is performed using waterfilling with a total power constraint (TPC). For the PPC design, we set a uniform power constraint $p_j = p_0\ \forall j$ for illustration. In Fig. 2, we show the average spectral efficiency obtained for both TPC and PPC designs. The performance of the proposed PPC design is close to that of the TPC design, yet there is a performance loss increasing with N_{s}. This effect comes from the difficulty of obtaining an accurate hybrid factorization when N_{s} increases, and from our pursuing an optimization of the Euclidean distance with per-antenna constraints, whilst the TPC design maximizes the spectral efficiency with a total power constraint. Fig. 3 shows the complementary cumulative distribution (CCDF) for the average power delivered to a given antenna. The proposed PPC design is shown to always meet the per-antenna constraints, yet not necessarily with equality. The TPC design yields a CCDF with larger variance across different antennas, which increases as N_{s} decreases. For instance, if a probability of 10^{-3} of not exceeding the maximum antenna budget is desired, the input power would need to be reduced by approximately 3 and 4.5 dB for the all-digital TPC design, which would shift the corresponding curves in Fig. 2 to the right by the same amount.

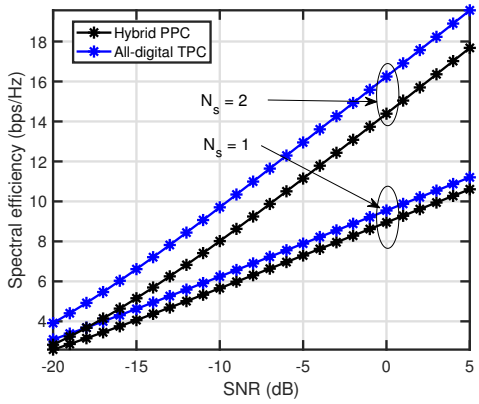

Fig. 2: Average spectral efficiency obtained with the proposed PPC and TPC designs. The number of transmit and receive antennas is $N_{\mathrm{t}} = 64$ and $N_{\mathrm{r}} = 16$, and the number of RF chains is $L_{\mathrm{t}} = 4$ and $L_{\mathrm{r}} = 2$.

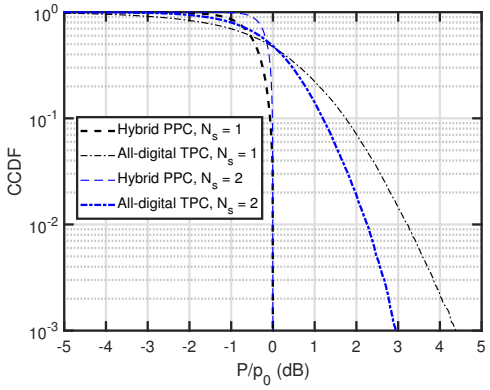

Fig. 3: Complementary Cumulative Distribution Function (CCDF) obtained with the proposed PPC and TPC designs. The number of transmit and receive antennas is $N_{\mathrm{t}} = 64$ and $N_{\mathrm{r}} = 16$, and the number of RF chains is $L_{\mathrm{t}} = 4$ and $L_{\mathrm{r}} = 2$.

5. CONCLUSIONS

In this paper, we developed a low-complexity solution to the problem of finding hybrid precoders and combiners maximizing spectral efficiency in a wideband OFDM/SC-FDE MIMO system with per-antenna power constraints. Despite the mathematical approximations adopted in our derivation, numerical results show the closeness of the proposed design method to that of the all-digital solution. Furthermore, we also showed the importance of considering per-antenna power constraints using the sample distribution of the power delivered to each antenna, highlighting that the per-antenna constraints are always met, yet not with equality in every case.

6. REFERENCES

[1] J. P. González-Coma, J. Rodríguez-Fernández, N. González-Prelcic, L. Castedo, and R. W. Heath, "Channel estimation and hybrid precoding for frequency selective multiuser mmwave MIMO systems," *IEEE Journal of Selected Topics in Signal Processing*, vol. 12, no. 2, pp. 353–367, May 2018.

[2] X. Yu, J. Zhang, and K. B. Letaief, "A hardware-efficient analog network structure for hybrid precoding in millimeter wave systems," *IEEE Journal of Selected Topics in Signal Processing*, vol. 12, no. 2, pp. 282–297, May 2018.

[3] J. Rodriguez-Fernandez and N. Gonzalez-Prelcic, "Low-complexity multiuser hybrid precoding and combining for frequency selective millimeter wave systems," *2018 IEEE 19th International Workshop on Signal Processing Advances in Wireless Communications (SPAWC)*, 2018.

[4] A. Alkhateeb and R. W. Heath Jr., "Frequency selective hybrid precoding for limited feedback millimeter wave systems," *IEEE Trans. Commun.*, vol. 64, no. 5, pp. 1801–1818, May 2016.

[5] S. Park, A. Alkhateeb, and R. W. H. Jr., "Dynamic Subarrays for Hybrid Precoding in Wideband mmWave MIMO Systems," *arXiv:1606.08405*, vol. abs/1606.08405, 2016.

[6] X. Yu, J. C. Shen, J. Zhang, and K. B. Letaief, "Alternating Minimization Algorithms for Hybrid Precoding in Millimeter Wave MIMO Systems," *IEEE Journal of Selected Topics in Signal Processing*, vol. 10, no. 3, pp. 485–500, April 2016.

[7] S. Park, A. Alkhateeb, and R. W. Heath, "Dynamic subarray architecture for wideband hybrid precoding in millimeter wave massive MIMO systems," in *2016 IEEE Global Conference on Signal and Information Processing (GlobalSIP)*, Dec 2016, pp. 600–604.

[8] W. M. Chan, T. Kim, H. Ghauch, and M. Bengtsson, "Subspace estimation and hybrid precoding for wideband millimeter-wave MIMO systems," in *2016 50th Asilomar Conference on Signals, Systems and Computers*, Nov 2016, pp. 286–290.

[9] A. Alkhateeb and R. W. Heath, "Gram schmidt based greedy hybrid precoding for frequency selective millimeter wave MIMO systems," in *2016 IEEE International Conference on Acoustics, Speech and Signal Processing (ICASSP)*, March 2016, pp. 3396–3400.

[10] P. L. Cao, T. J. Oechtering, and M. Skoglund, "Precoding design for massive MIMO systems with sub-connected architecture and per-antenna power constraints," in *WSA 2018; 22nd International ITG Workshop on Smart Antennas*, March 2018, pp. 1–6.

[11] R. López-Valcarce, N. González-Prelcic, C. Rusu, and R. W. Heath, "Hybrid precoders and combiners for mmwave MIMO systems with per-antenna power constraints," in *2016 IEEE Global Communications Conference (GLOBECOM)*, Dec 2016, pp. 1–6.

[12] J. Rodríguez-Fernández, R. López-Valcarce, and N. González-Prelcic, "Hybrid precoding and combining for frequency-selective mmwave MIMO systems with per-antenna power constraints," *available at arXiv*, 2018.

[13] P. Schniter and A. Sayeed, "Channel estimation and precoder design for millimeter-wave communications: The sparse way," in *Proc. Asilomar Conf. Signals, Syst., Comput.*, Nov 2014, pp. 273–277.

[14] J. Rodríguez-Fernández, N. González-Prelcic, K. Venugopal, and R. W. Heath, "Frequency-domain compressive channel estimation for frequency-selective hybrid millimeter wave MIMO systems," *IEEE Transactions on Wireless Communications*, vol. 17, no. 5, pp. 2946–2960, May 2018.

[15] J. von Neumann, "Some matrix inequalities and metrization of matrix-space," *Tomsk. Univ. Rev.*, vol. 1, pp. 286–300, 1937.

[16] G. H. Golub and C. F. van Loan, "Matrix computations, 3rd ed." *Johns Hopkins Univ. Press*, 1996.

[17] 3GPP, "Study on channel model for frequencies from 0.5 to 100 GHz (release 14)," *Tech. Rep. v14.1.1*, 2017.

[18] S. Jaeckel, L. Raschkowski, K. Brner, and L. Thiele, "QuaDRiGa: A 3-D Multi-Cell Channel Model With Time Evolution for Enabling Virtual Field Trials," *IEEE Transactions on Antennas and Propagation*, vol. 62, no. 6, pp. 3242–3256, June 2014.

[19] S. Jaeckel, L. Raschkowski, K. Brner, L. Thiele, F. Burkhardt, and E. Eberlein, "QuaDRiGa: QuaDRiGa - Quasi Deterministic Ratio Channel Generator, User Manual and Documentation," *Fraunhofer Heinrich Hertz Institute, Tech. Rep. v2.0.0*, 2017.